12th Asia-Pacific Conference on Combustion,
Fukuoka International Congress Center, Fukuoka, Japan
1st -5th July 2019.

Direct numerical simulations of the ignition of temporally evolving *n*-heptane jet under RCCI combustion-relevant conditions

Gwang Hyeon Yu[1], Minh Bau Luong[2], Suk Ho Chung[2], Chun Sang Yoo[1,*]

[1]Department of Mechanical Engineering, Ulsan National Institute of Science and Technology
Ulsan, 44919, Republic of Korea

[2]Clean Combustion Research Center, King Abdullah University of Science and Technology
Thuwal, Saudi Arabia

Abstract

The ignition characteristics of a temporally evolving *n*-heptane jet under reactivity controlled compression ignition (RCCI) conditions are investigated using 2-D direct numerical simulation with a 116-species PRF reduced mechanism. For RCCI combustion, *n*-heptane and *iso*-octane are selected as two different fuels that have opposite ignition characteristics. In real engine, relatively-low reactivity fuel is delivered by port-fuel injection and relatively-high reactivity fuel is directly injected. Thus, the ignition characteristics of temporally evolving jet can be investigated with different jet velocity, U_0. It is found that the first-stage ignition kernels occur within *n*-heptane jet near the mixing layer and develop into low temperature flame, propagating into relatively fuel-rich mixture of *n*-heptane jet. The high temperature ignition kernel is also formed in the *n*-heptane jet, and then rapidly propagate into both relatively fuel-rich *n*-heptane jet and fuel-lean *iso*-octane/air mixture. Finally, the end-gas autoignition occurs. It is also found that the first- and second-stage ignitions occur quickly with increasing U_0; the overall combustion is prolonged and the peak of heat release rate is reduced with increasing U_0.

1 Introduction

In recent decades, numerous experimental and numerical researches on next generation engines have been performed. This is because the conventional IC engines emit air pollutants such as NOx and soot. Therefore, it is necessary to develop a novel engine that can resolve the air-pollution issues. As one of next-generation IC engines, homogeneous-charge compression ignition (HCCI) engines have been spotlighted. The HCCI engine as one of low temperature combustion (LTC) engines uses highly diluted, lean, well-mixed fuel/air mixture and operates under a high compression ratio to achieve a higher thermal efficiency. Therefore, the HCCI engine can provide high thermal efficiency like diesel engine and significantly reduce the NOx and pollutant emission without any high price after-treatments [1].

Although the HCCI engine has many advantages over the conventional IC engines, it still has problems for commercialization. There are two major reasons: excessive pressure rise rate (PRR) and difficulty in ignition-timing control. Since the HCCI engine uses a well-mixed fuel/air charge, the ignition delays of in-cylinder mixture are almost the same. This leads to simultaneous auto-ignition, resulting in the excessive PRR. Moreover, the HCCI engine has no direct method to control ignition timing such as spark plug or fuel injection, and hence, HCCI combustion starts only by compression heating due to the piston motion. Therefore, the chemical kinetics of the fuel/air mixture governs the overall ignition timing of HCCI combustion. Various in-cylinder conditions such as pressure, temperature, fuel composition, reactivity, and equivalence ratio can affect chemical kinetics.

To resolve the excessive PRR due to simultaneous auto-ignition, various methods have been proposed. Among them, reactivity controlled compression ignition (RCCI) combustion has been found to be able to control the ignition timing and combustion duration more effectively [3]. Numerous experimental and numerical studies of RCCI combustion have been conducted [1-7]. Especially, in our previous studies [8, 9], the numerical simulations of RCCI and SCCI combustion were conducted by varying r and u' at different T_0. It was found from the study that, the PRF number stratification, PRF′, in RCCI combustion has a dominant effect on the overall combustion within the negative temperature coefficient (NTC) regime.

In the previous numerical studies, it was assumed that all the in-cylinder injections are finished and injected fuel/air mixture is well mixed before the piston reaches top dead center (TDC). Then, the initial conditions are specified based on TDC in-cylinder parameters. Under such assumptions, the overall simulation time could be reduced and the fundamental ignition mechanism could be elucidated. However, the ignition characteristics during the injection or right after the injection could not be investigated. When fuel is directly injected, injected fuel and in-cylinder fuel/air mixture generates mixing layer because of injection velocity. This mixing layer affect the whole ignition process, however, the effects of the mixing layer on the HCCI combustion were not fully understood. Recently, Krisman et al. [10, 11] numerically investigated the combustion characteristics of diesel-relevant conditions. At this study the DME and air mixture are used and initial mixing layer exist. It was found that low temperature combustion significantly affects high temperature combustion and the ignition occurred as a multi-stage and multi-mode process.

Therefore, the objective of the present study is to investigate the fundamental ignition characteristics of primary reference fuel (PRF)/air mixtures with mixing layer under RCCI condition

Corresponding author. Fax: +52-217-2409, +51-629-6126
E-mail address: csyoo@unist.ac.kr, jeongpark@pknu.ac.kr

using 2-D DNSs. We focus on two main points: (1) the fundamental ignition mechanism of RCCI combustion with mixing layer, and (2) the initial shear velocity effects on the overall RCCI combustion.

2 Numerical method and initial conditions

The Sandia DNS code, S3D, was used to solve the compressible Navier-Stokes, species continuity, and total energy equations for the ignition of PRF/air mixture. A fourth-order explicit Runge-Kutta method and an eight-order central difference scheme were employed for time integration and spatial discretization, respectively. Periodic boundary conditions were imposed in all directions. To account the compression heating and expansion cooling effects by piston motion, including mass source term in the governing equation. For details of the compression heating/cooling model, readers are referred to [4].

The 116-species PRF/air reduced mechanism for PRF oxidation was adopted to simulate the RCCI combustion. The reduced mechanism was validated through a wide range of PRF composition, pressure, and temperature conditions. The relevant engine specifications are in [4]. For all DNSs, to reduce the computational cost, the simulations start at -25°CA ATDC, which the injections of *iso*-octane and *n*-heptane are assumed to be already finished. According to the motored pressure trace with an intake pressure of 1.0 atm (not shown here), the initial mean pressure, p_0, and mean temperature, T_0, and the mean equivalence ratio, ϕ_0, are set to be 18.2 atm, 720 K, and 0.45, respectively. The mean fuel is PRF50. In real RCCI engine, two different fuels are injected by two different injection methods. The low reactivity fuel/air mixture is supplied by port-fuel injector (PFI) and high reactivity fuel is directly-injected by direct injector (DI). Since low reactivity fuel/air mixture is injected at early crank angle, the charge is homogeneously distributed whole engine cylinder, whereas high reactivity fuel is injected at near TDC, the fuel generates inhomogeneities in equivalence ratio and temperature.

To reproduce the mixing layer, the relative velocity, temperature, and species composition of the *n*-heptane jet are specified by a top-hat shaped profile function described by:

$$f(y) = \tfrac{1}{2}\left[\tanh\left(y-\tfrac{2}{5}H\right)/\sigma - \tanh\left(y-\tfrac{3}{5}H\right)/\sigma\right], \quad (1)$$

Figures 1 and 2 shows the initial conditions of 2-D DNS and the schematic diagram of the domain configuration. As shown in Figure 1, the temperature of *iso*-octane/air mixture is 740 K and the mean temperature of *n*-heptane is 590 K and the temperature fluctuation, T', is 20 K. Note that the fluctuation of T is carefully chosen to match those from experiments as in [7]. Due to evaporative cooling of directly injected fuel, negatively-correlated (NC) $T-\phi$ distribution can exist at the *n*-heptane fuel. From the experimental study in [12], the range of ϕ is about 0.2-2.0, similar ϕ range is accounted on this study. As such, the distribution of T and ϕ lies in the optimal range for RCCI combustion to maintain low-temperature combustion with ultra-low emissions [5, 6]. To investigate the effect of shear velocity, three different DNSs cases are performed with varying shear velocity, 0, 5, and 10, respectively. The initial parameter of each DNS case represented in Table 1.

* Corresponding author. Fax: +82-52-217-2449
E-mail address: csyoo@unist.ac.kr

The most energetic length scales of turbulence, temperature and concentration, l_e, l_{T_e}, l_{m_e} are 1.2 mm is specified for all DNSs. In real HCCI engine, the turbulence time scale, τ_t, is comparable to τ_{ig}^0, ($\tau_t/\tau_{ig}^0 \sim O(1)$). Thus, the turbulence intensity, u', of 0.4 is deliberately selected to ensure that the turbulence time scale, $\tau_t = l_e/u'$, of 3.0 ms.

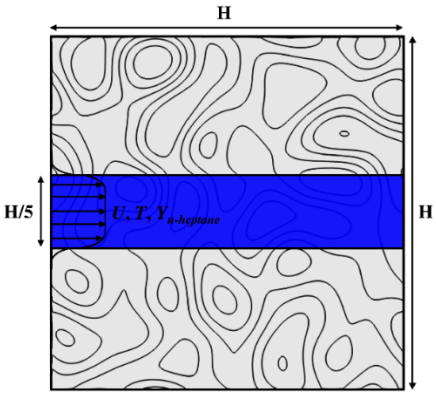

Figure 1: Schematic diagram of the domain configuration with the boundary and initial conditions.

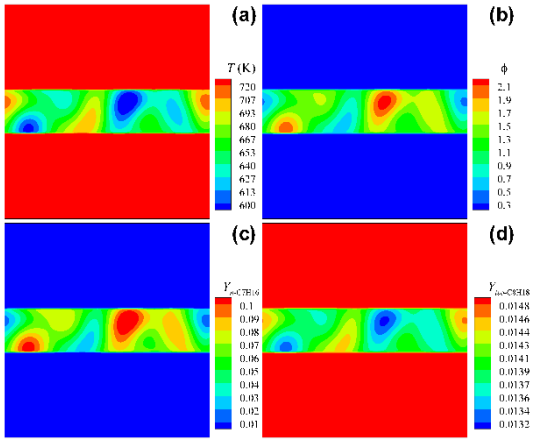

Figure 2: Initial T, ϕ, *n*-heptane and *iso*-octane mass fraction fields of Case 1.

Table 1: Initial parameters of 2-D DNS cases.

Case	U_0 (m/s)	ϕ_0	T_{oct} (K)	T_{hep} (K)	T'_{hep} (K)	l_e (mm)	u' (mm)
1	0.0	0.45	740	650	20	1.2	0.4
2	5.0	0.45	740	650	20	1.2	0.4
3	10.0	0.45	740	650	20	1.2	0.4

A 2-D computational domain of 3.2 x 3.2 mm^2 discretized with 2560 grids points in each direction was used for all 2-D DNSs. The coarse grid resolution of 1.25 μm with a time step of 2.5 *n*s is required to resolve thin flame fronts. The 2-D DNSs were performed on a Cray XC40 system at King Abdullah University of Science and Technology (KAUST). Each of the DNSs consumed approximately 1.0 million CPU-hours.

3 Results and discussion

Figure 3 shows the instantaneous isocontours of normalized heat release rate (HRR) fields at each time step of Case 1 and 3. The

HRR normalized by 100 J/mm^{3}s. Ans also we adopted a mixture fraction, ξ, that is calculated based on the nitrogen mass fraction, Y_{N_2}, ranging from zero at the *iso*-octane/air mixture to 1.0 at the *n*-heptane jet as in [11]:

$$\xi = \frac{Y_{N_2} - Y_{N_2}^{\mathrm{oct}}}{Y_{N_2}^{\mathrm{hep}} - Y_{N_2}^{\mathrm{oct}}}, \tag{2}$$

where the superscript 'oct' and 'hep' represent the *iso*-octane/air mixture and the *n*-heptane jet, respectively. ξ =0.1 isoline represent the middle of mixing layer which separates the *iso*-octane and *n*-heptane jet. As such, we assume that if $\xi > 0.1$, the heat is released from the *n*-heptane jet and if $\xi < 0.1$, heat is released from the *iso*-octane/air mixture.

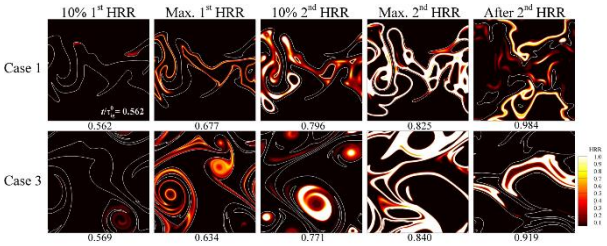

Figure 3: Instantaneous isocontours of normalized HRR fields at the each time step of Cases 1 and 3.

Several points are noted from Fig. 3. First, several low temperature ignition kernels occur near the mixing layer during the early phase of the first-stage ignition (see the first column). The ignition kernels develop where the scalar dissipation rate, χ, is very low (not shown here) similar to previous work [11, 12]. The scalar dissipation rate is defined by $\chi = 2D|\nabla\xi|^2$, where D is the thermal diffusivity. At a times later (see the second column), additional low temperature ignition kernels develop and merge with each other. And kernels become low temperature flame and propagate into fuel-rich mixtures inside of the *n*-heptane jet. During the early phase of the second-stage ignition (see the third column), several high temperature ignition kernels form and merge with each other, developing into high temperature flame. They propagate into fuel-lean mixtures following the trajectories of low temperature flames. At the second-stage ignition, the high temperature flames propagate into the *iso*-octane/air mixture. For Case 1, the high temperature flames keep consuming the remaining *n*-heptane. Finally, the remaining *iso*-octane/air mixture auto-ignite simultaneously (see the fifth column), which is the end-gas auto-ignition of the HCCI combustion.

Figure 4 shows the temporal evolution of mean temperature and mean HRR for 0-D, and 2-D simulation. Several points are noted from Fig 4. First, the first-stage ignition is advanced in time and the peak of mean HRR is increased with increasing shear velocity. This result is different from previous studies in which turbulence with large u' was found to effectively homogenize fuel/air mixture, and thus, the first- and second-stage ignitions are delayed and the peak of mean HRR is decreased with increasing u'. Second, the second-stage ignition is advanced in time and the duration of heat release rate is increased with increasing shear velocity. However, the peak of mean HRR shows non-monotonic behavior. Third, for Case 1 and 2, the third peak of HRR occurs. As shown in Fig 3, this HRR is from *iso*-octane/air mixture.

To understand the ignition characteristics of the *n*-heptane and *iso*-octane separately, we evaluate mean values based on the mixture fraction. Figure 5 shows the temporal evolutions of the mean temperature and HRR for *n*-heptane jet and *iso*-octane/air mixture. It is readily observed that during the first-stage ignition, almost heat is released from *n*-heptane jet. From this, we can ensure that *n*-heptane oxidation governs the first-stage ignition characteristics of the system. The peak of second-stage HRR is decreased with increasing shear velocity, and also, the third peak of HRR for Case 3 is observed.

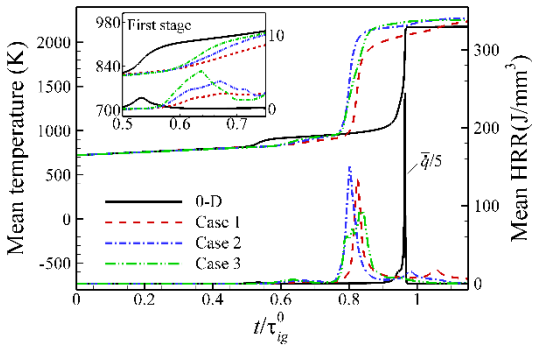

Figure 4: Temporal evolution of the mean temperature and HRR for different shear velocity cases with the corresponding 0-D ignition of PRF50/air mixture.

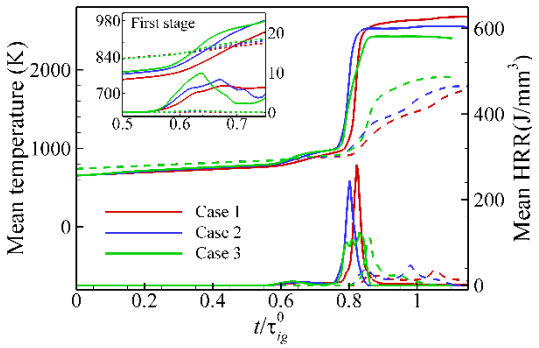

Figure 5 shows the temporal evolutions of the mean temperature and HRR and for *n*-heptane jet and *iso*-octane/air mixture.

4 Conclusions

2-D DNSs of the ignition of a lean PRF/air mixture with a mixing layer under RCCI combustion-relevant condition were performed with a 116-species PRF reduced mechanism by varying the shear velocity, U_0. For the DNSs, we adopted a compression heating model to account for the compression heating and expansion cooling effect of the real engine. It was found that during the first-stage ignition, low-temperature ignition kernels are formed first near the mixing layer and develop into low temperature flames. Subsequently, they propagate into relatively fuel-rich region. As a result, the main combustion starts at the fuel-rich region. The high temperature flames develop and propagate into fuel-lean mixture. After the consumption of *n*-heptane jet, the flames propagate into *iso*-octane/air mixture. Finally, the remaining *iso*-octane/air mixture auto-ignite simultaneously. It was also found that the first-stage ignition is advanced in time and the peak of mean HRR is increased with increasing shear velocity. On the other hand, the second-stage ignition is also advanced in time and the peak of mean HRR is decreased and the duration is prolonged with increasing shear velocity. These results suggest that the the mixing layer velocity can also control the excessive PRR and the ignition timing.

5 Acknowledgments

This research was supported by Basic Science Research Program

through the National Research Foundation of Korea (NRF) funded by the Ministry of Science, ICT & Future Planning (NRF-2018R1A2A2A05018901). This research used the resources of the KAUST Supercomputing Laboratory and the UNIST Supercomputing Center.

References

[1] J. E. Dec, *Proc. Combust. Inst.* **32** (2009) 2727-2742.

[2] S. L. Kokjohn, R. M. Hanson, D. A. Splitter, R. D. Reitz, *Int. J. Engine* **12** (2011) 209-226.

[3] R. D. Reitz, G. Duraisamy, *Prog. Energy Combust. Sci.* **46** (2015) 12-71.

[4] M. B. Luong, R. Sankaran, G. H. Yu, S. H. Chung, C. S. Yoo, *Combust. Flame* **183** (2017) 309-321.

[5] S. L. Kokjohn, R. D. Reitz, D. A. Splitter, M. Musculus, *SAE paper* (2012) 2012-01-0375.

[6] S. L. Kokjohn, M. P. B. Musculus, R. D. Reitz, *Combust. Flame* **162** (2015) 2729-2742.

[7] J. E. Dec, W. Hwang, *SAE Trans. Paper* (2009) 2009-01-0650.

[8] M. B. Luong, G. H. Yu, S. H. Chung, C. S. Yoo, *Proc. Combust. Inst.* **36** (2017) 3587-3596.

[9] M. B. Luong, G. H. Yu, S. H. Chung, C. S. Yoo, *Proc. Combust. Inst.* **36** (2017) 3623-3631.

[10] A. Krisman, E. R. Hawkes, M. Talei, A. Bhagatawala, J. H. Chen, *Combust. Flame* **172** (2016) 326-341.

[11] A. Krisman, E. R. Hawkes, M. Talei, A. Bhagatawala, J. H. Chen, *Proc. Combust. Inst.* **36** (2017) 3567-3575.

[12] Q. Tang, H. Liu, M. Li, M. Yao, Z. Li, *Combust. Flame* **177** (2017) 98-108.